Low Cycle Fatigue in Rene 88DT at 650 °C: Crack Nucleation Mechanisms and Modeling

KIP O. FINDLEY and ASHOK SAXENA

Intermediate-temperature low-cycle-fatigue experiments were conducted on three microstructural conditions of the nickel-base superalloy Rene 88DT over several strain ranges. The most significant difference between the microstructural conditions was the grain size; two of the conditions had an average grain diameter of approximately 20 μm, while the third condition had an average grain diameter of 6 μm. Two dominant crack nucleation mechanisms were observed on the specimen fracture surfaces: crack nucleation from surface slip band damage accumulation and crack nucleation around subsurface inclusion clusters. The experimental results indicate that both the grain size and the applied strain range are contributing factors in the prevailing crack nucleation mechanism. The Fatemi-Socie parameter, a multiaxial fatigue damage parameter, was used to examine the ease and probability of surface slip band crack nucleation for these microstructural conditions. The parameter was modified to explicitly include grain size, fatigue R-ratio, and applied strain range, thus giving it a more physically meaningful basis. This modified Fatemi-Socie parameter was found to be a suitable parameter for characterizing the ease of surface slip band cracking for materials with different grain sizes and is able to explain the observed disparity in fatigue lives based on microstructural design.

I. INTRODUCTION

CRACK nucleation in low- and high-cycle-fatigue conditions has been attributed to various mechanisms in nickel-base superalloys. Defects, arising from the powder metallurgy processing and including ceramic inclusion particles and pores and voids, have been observed to nucleate dominant cracks in several Ni-base superalloys in low cycle fatigue (LCF) conditions at elevated temperatures.[1–5] Crack nucleation due to plastic damage accumulation within a surface slip band has also been observed by several authors at room temperature and elevated temperature conditions.[5,6,7]

There is seemingly a competition between crack nucleation from surface slip band cracking and crack nucleation from defects in the material. The processing history and resulting microstructure of the alloy often governs which crack nucleation mechanism prevails. Alexendre *et al.*[5] found that cracks generally nucleated from slip band cracking in INCONEL* 718 with comparatively large grain sizes, whereas cracks nucleated from inclusion particles when the material grain size was comparatively small. Caton *et al.*[4] performed LCF experiments on RENE 88DT** at low applied strain ranges at elevated temperature and found that most of the cracks nucleated from the subsurface of the specimens; they nucleated either from inclusion particles or from crystallographic features.

*ICONEL is a trademark of Special Metals Corporation, New Hartford, NY.

**RENE 88DT is a trademark of General Electric Aircraft Engines, Cincinnati, OH.

KIP O. FINDLEY, Undergraduate Research Professor, is with the School of Mechanical and Materials Engineering, Washington State University, Pullman, WA 99163. Contact e-mail: kfindley@wsu.edu ASHOK SAXENA, Dean and Distinguished Professor, is with the College of Engineering, University of Arkansas, 4183 Bell Engineering Center, Fayetteville, AR 72701.

Manuscript submitted July 5, 2005.

The first objective of this study is to characterize the crack nucleation mechanisms prevalent in LCF conditions at 650 °C in Rene 88DT with applied strain ranges that vary from below to well above the cyclic yield strain of the material for multiple microstructure conditions. The effect of applied strain range and microstructure on the resulting crack nucleation mechanism is discussed.

It is also essential to develop a quantitative understanding to predict the LCF crack nucleation behavior through a physically based model to reduce the scatter in LCF data associated with competing crack nucleation mechanisms. Thus, the second objective of this study is to explore the use of a parameter known as the Fatemi-Socie parameter to model crack nucleation in slip bands and also to explain the considerable difference in LCF properties of Rene 88DT material with different average grain sizes. A quantitative model for crack nucleation due to subsurface inclusions will be considered in a future paper.

II. EXPERIMENTAL PROCEDURE

Three microstructural conditions of the nickel-base superalloy Rene 88DT, a commonly used powder metallurgy aircraft engine disk material, were studied. Rene 88DT is a polycrystalline, equiaxed material mainly consisting of an fcc matrix phase γ, an $L1_2$-type ordered strengthening precipitate γ', and several carbide and boride phases. The three microstructural conditions that were produced for experiments will henceforth be labeled conditions N, O, and P. Conditions N and O were produced by homogenizing the material above the solvus temperature and then cooling in a two-step process to room temperature, which was followed by intermediate temperature aging at 760 °C; the transition temperature between the first and second steps of the cooling process was 1038 °C. The only difference between the heat treatments for the N and O condition was the first-step cooling rate: the cooling rate for the N condition was 8.3 °C/min and 3.3 °C/min for the O condition. The fracture surfaces, data, and material for condition P came

from the research sponsor, and the heat treatment for the microstructural condition is proprietary. To characterize the microstructure, planar metallographic specimens were obtained for each condition. They were mechanically ground and polished, with the final step being a light polish on a colloidal silica media. A solution containing 95 parts HCl, 3 parts H_2O_2, and 2 parts HNO_3 was used to etch grain boundaries in the material. A glycerol-based etchant comprising 3 parts glycerol, 3 parts HCl, 1 part HNO_3, and 1 part HF was used to etch the γ' precipitates.

The γ' size distribution and grain size were found to vary between the three conditions. A summary of the three microstructural conditions, including grain size and the larger cooling γ' size and spacing, is shown in Table I. The cooling γ' size distribution and first nearest neighbor distance (NND) are very similar for the three microstructure conditions. However, the average grain diameter for conditions N and O (20 to 21 μm) is much larger than the average grain diameter for condition P (6 μm). The difference in grain size results in significant disparities between the three conditions in the dominant crack nucleation mechanism, which will be addressed later in this article. The similarity between the N and O microstructural conditions can be attributed to minor variation in their first-step cooling rates.

Strain-controlled, uniaxial LCF experiments were performed on round bar specimens from the three conditions at an intermediate temperature of 650 °C using a servo-hydraulic test frame. The objective of these experiments was to compare the cyclic stress–strain behavior between the three conditions and to observe the relationship between applied strain range, crack nucleation mechanisms, and resulting fatigue lives for each microstructure condition. Specimens from conditions N and O were tested with $R = -1$ and applied strain ranges of 0.66 pct, 0.75 pct, and 1.5 pct, whereas specimens from condition P were tested with $R = 0$ and applied strain ranges of 0.66 pct, 0.79 pct, 0.94 pct, and 1.15 pct. The diameter in the gage section was 6.35 mm in the N and O condition specimens and 10.16 mm in the P condition specimens. The frequency varied from 20 to 30 cycles per minute, and the temperature was controlled to ±3 °C within the gage section using induction heating and was monitored by thermocouples placed outside the gage section of the specimens. To avoid artificially induced crack nucleation from the conical points of a high-temperature extensometer, an MTS model 632.06 displacement gage (''one-arm bandit'') was used to measure load-line displacement on the test actuator during the experiment. Dummy specimens were used to calibrate the maximum and minimum values of the desired strain ranges measured by a high-temperature extensometer within the specimen gage section to the corresponding displacement values measured by the one-arm bandit. The experiments were generally terminated when there was a 5 pct load drop from the saturation load range. The specimens were then fractured in high-cycle-fatigue conditions with $R = 0.1$ at room temperature to observe the fracture surfaces.

The regions on the fracture surfaces where cracks nucleated and the surrounding regions in the specimen gage section were examined using a LEICA* MZ6 stereoscope, a Leica optical microscope, and LEO 1530 thermally assisted field emission scanning electron microscope (SEM).

*LEICA is a trademark of Leica Microsystems Inc., Bannookborn, IL.

Table I. Summary of the Grain Size and γ' Size and Spacing in the Three Microstructural Conditions

	Grain Size (μm)	γ' Volume Fraction (pct)	γ' Average Diameter (μm)	γ' Average NND (μm)
N	21	21	0.258	0.383 ± 0.148
O	20	20	0.28	0.342 ± 0.156
P	6	22	0.27	0.345 ± 0.106

Table II. Comparison of the Cycles to Failure and Fatigue Stress-Strain Behavior for Specimens from the Three Conditions Tested at $\Delta\varepsilon = 0.66$ pct and $\Delta\varepsilon = 0.75$ pct to 0.79 pct and 650 °C

Condition	Strain Range	Cycles to Failure	Half Life Stress Range (MPa)
N	0.0066	58550	1241
	0.0066	22210	1276
	0.0066	25000	1324
O	0.0066	98475	1351
	0.0066	16915	1358
	0.0066	44070	1310
P	0.0066	491180	1255
	0.0066	928420	1248
	0.0066	977060	1241
N	0.0075	4680	1448
	0.0075	5500	1462
O	0.0075	11075	1475
	0.0075	5080	1510
P	0.0079	139150	1448
	0.0079	182200	1455
	0.0079	197570	1448

III. LOW CYCLE FATIGUE TESTING RESULTS

Some interesting comparisons can be made for the saturation or half-life stress ranges and the fatigue lives for specimens from the three conditions tested with the various applied strain ranges. Table II shows data collected from the three conditions for similar applied strain ranges. For $\Delta\varepsilon = 0.66$ pct and $\Delta\varepsilon = 0.75$ to 0.79 pct, the half-life stress range values for the three conditions are very similar; however, the number of cycles to failure for conditions N and O are more than an order of magnitude smaller than the number of cycles to failure for condition P. There is significant scatter in the cycles to failure at comparable strain ranges for all three conditions. These comparisons suggest that the processing conditions and resulting microstructural differences between the conditions have little effect on the macroscopic fatigue stress–strain properties. However, the observed disparity in fatigue lives between conditions N and O *vs* P suggest that the microstructure strongly influences the number of cycles to failure. Since the γ' size distributions are very similar for the three conditions, the grain size, which is a factor of 3 smaller in condition P than in conditions N and O, probably has the greatest effect on the fatigue life, which will be discussed in detail later. It could also be expected the

P condition specimens, with R = 0, would have a shorter fatigue life than the N and O specimens with R = −1; however, the results indicate that fatigue life is more sensitive to grain size than the loading ratio.

IV. CHARACTERIZATION OF THE CRACK NUCLEATION MECHANISMS

Two crack nucleation mechanisms were observed from the fracture surfaces: cracks nucleating at subsurface inclusion clusters and cracks nucleating due to plastic damage accumulation within slip bands on the specimen surface; these mechanisms are consistent with observations in literature for intermediate-temperature crack nucleation in nickel-base superalloys.[1–7] All of the fracture surfaces exhibit obvious oxidation patterns that define the crack growth and indicate the region of crack nucleation. Figure 1 shows a low-magnification stereoscope image from an N condition specimen tested with $\Delta\varepsilon = 0.66$ pct, where the oxidation pattern outlines crack growth from the specimen surface. Figure 2 shows where a crack nucleated in the specimen subsurface in a P condition specimen tested with $\Delta\varepsilon = 0.79$ pct; again, the oxidation pattern effectively outlines the crack nucleation region. The location of the crack nucleation site was generally indicative of the crack nucleation mechanism. Cracks that originate on the surface are due to plastic damage accumulation within slip bands, whereas crack nucleation in the subsurface occurs around an inclusion or inclusion cluster.

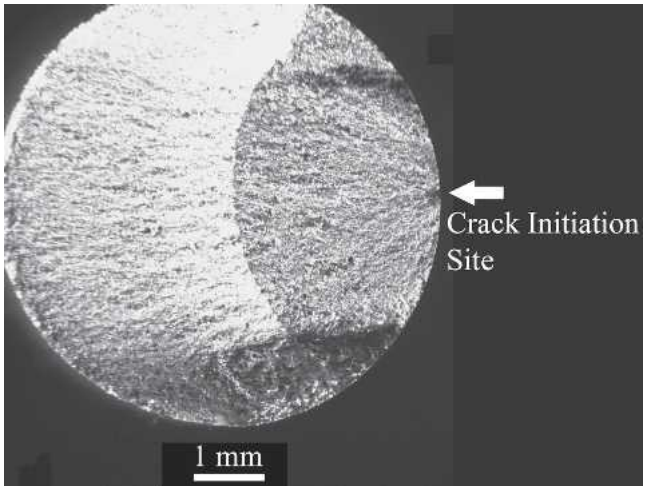

Fig. 1—Stereoscope image of an N condition specimen tested with $\Delta\varepsilon = 0.66$ pct at 650 °C.

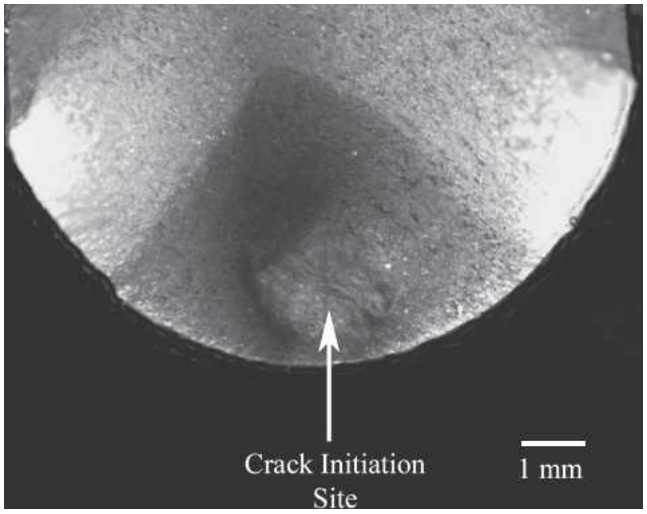

Fig. 2—Stereoscope image of a P condition specimen tested with $\Delta\varepsilon = 0.79$ pct at 650 °C.

The SEM image in Figure 3, corresponding to the fracture surface shown in Figure 1 and representative of surface crack nucleation from damage accumulation within slip bands, shows the region of crack nucleation and short crack growth. Radial or ''river-pattern'' lines point back to the crack nucleation site, which is in the proximity of the specimen surface. Faceted crack growth is also evident in the region and defines a typical ''thumbnail'' crack. Surface slip band crack nucleation is prevalent for all of the N and O condition specimens and a portion of the P condition specimens. A crack nucleation region for an N condition specimen tested with $\Delta\varepsilon = 0.75$ pct is shown in Figure 4. In this SEM image, however, the specimen is tilted approximately 90 deg so the electron beam is normal to the surface of the round bar gage section in the vicinity of the crack nucleation region. The image shows that the crack nucleation site is oriented 30 to 45 deg from the loading axis. This is consistent with findings by Boyd-Lee and King[6] and Healy *et al.*,[7] who observed crack nucleation due to slip band cracking where the nucleation sites were oriented between 30 and 60 deg from the loading axis, with the most common orientation being between 40 and 45 deg. Slip band cracking is a logical conclusion from these observations because the maximum shear stress or strain, which is responsible for plastic deformation in the material, is at an orientation of 45 deg from the loading axis. Furthermore, there is no evidence on the fracture surface of the specimens shown in Figures 1, 3, or 4 of a defect such as a void or inclusion particle being associated with crack nucleation.

Evidence of slip band cracking is also present on the surfaces of the round bar specimens in the proximity of the crack nucleation region. One of the broken halves of several of the LCF specimens was mounted in epoxy with

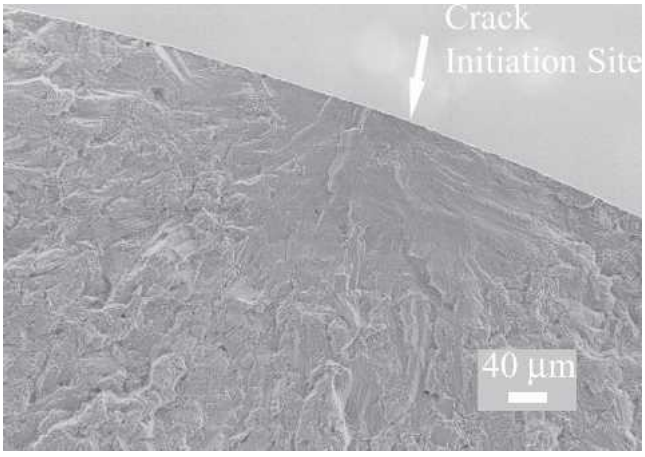

Fig. 3—SEM image of an N condition specimen tested at $\Delta\varepsilon = 0.66$ pct and 650 °C, showing the crack nucleation region.

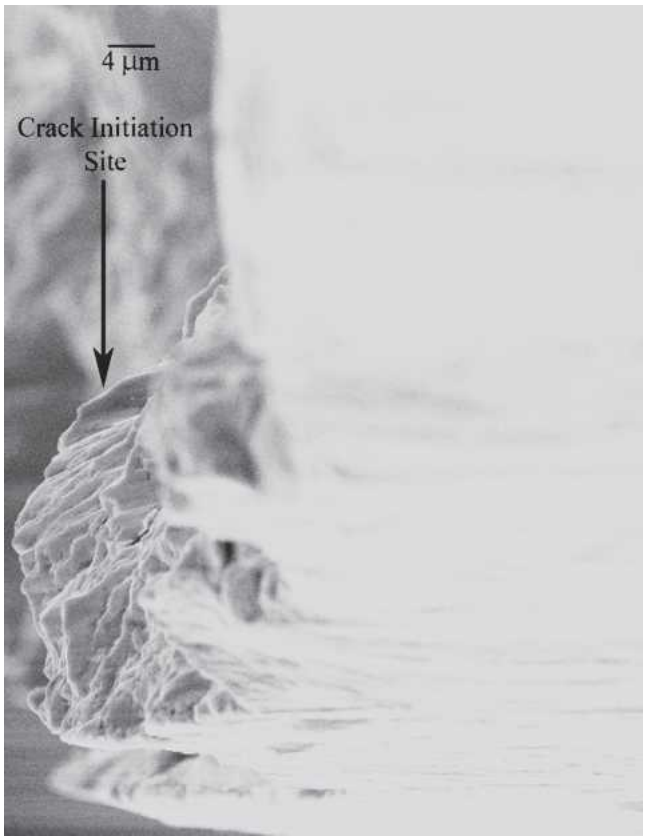

Fig. 4—SEM image of a specimen tested at $\Delta\varepsilon = 0.75$ pct and 650 °C tilted so the surface of the gage section of the specimen is normal to the electron beam in the vicinity of the crack nucleation site.

the surface of the round bar normal to the flat surface of the mount. The exposed area of the surface of the round bar, which was lightly polished to produce a small flat area suitable for optical microscope imaging, included the crack nucleation region. Figure 5 shows one such image taken from an O condition specimen tested with $\Delta\varepsilon = 0.75$ pct. The image clearly shows a large crack that nucleated and grew between 30 and 60 deg from the loading direction and intersects the fracture surface in the crack nucleation region. In addition, side branches emanate perpendicular to the major crack and the lowest branch becomes a crack of comparable size. The orientation of these cracks with respect to the loading direction and the orthogonal nature of the major cracks and side branches provide evidence of slip band cracking on orthogonal slip systems such as the {111}<110> family, which would be the most favorable slip system in Rene 88DT. Cracks with similar orientations are prominent in the gage sections of the specimens where slip band crack nucleation occurred.

The other prominent crack nucleation mechanism involved cracks nucleating around inclusion particles, generally in the subsurface of the round bar specimens. These particles most likely contaminate the material during powder metallurgy processing, and their size is limited by the mesh size used during powder processing. These particles are often brittle in nature and have a different coefficient of thermal expansion than the matrix material, as well as very little coherency with the matrix, making them probable locations for crack nucleation.

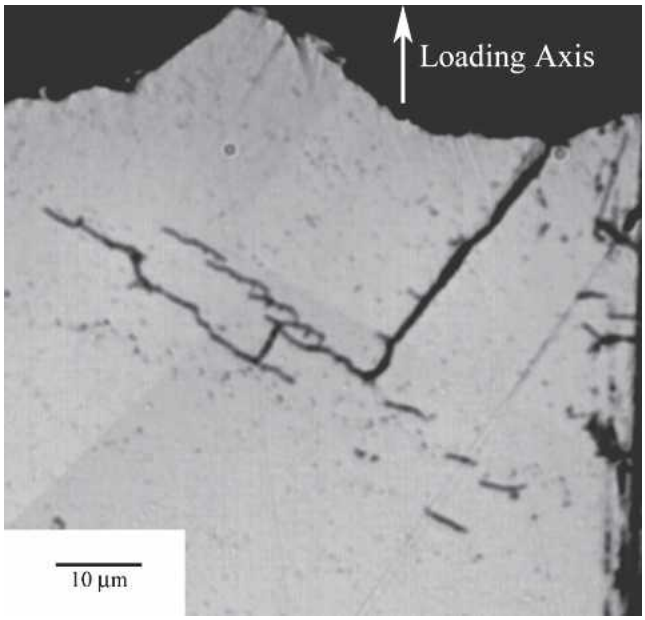

Fig. 5—A polished area of the gage section in the region of crack nucleation for an O condition specimen tested at $\Delta\varepsilon = 0.75$ pct at 650 °C.

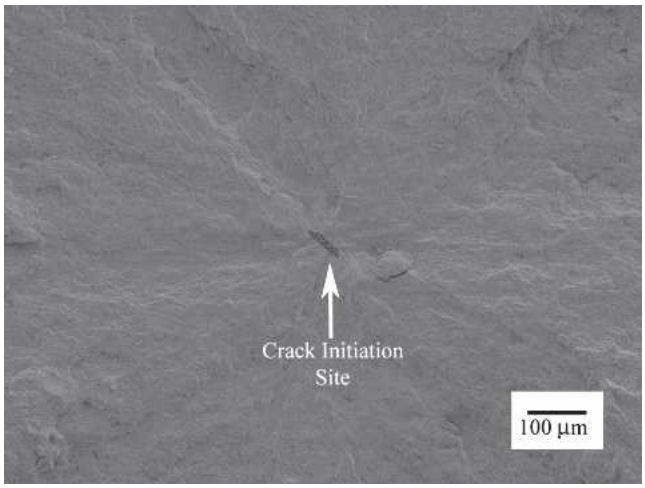

Fig. 6—Aluminum oxide inclusion cluster on the fracture surface of a P condition specimen tested at $\Delta\varepsilon = 0.79$ pct and 650 °C.

Inclusion-related failures were generally observed to originate in the LCF specimen subsurface, as shown in Figure 2. The major dimension of the inclusion clusters varied between 40 and 120 μm on these fracture surfaces. Figure 6 shows an SEM image of the crack nucleation region around an inclusion cluster where radial or ''river-pattern'' lines point back to a cluster of particles. Figure 7 is a higher-magnification image that shows the inclusion cluster in detail. Energy-dispersive spectroscopy (EDS) analysis on the particle cluster revealed that the particles were most likely aluminum oxide defects, which is consistent with the findings of other research.[8]

Dominant cracks that originated from this mechanism were observed only in the P condition specimens. The major microstructural difference between the three conditions is the grain size, which suggests that grain size is an important

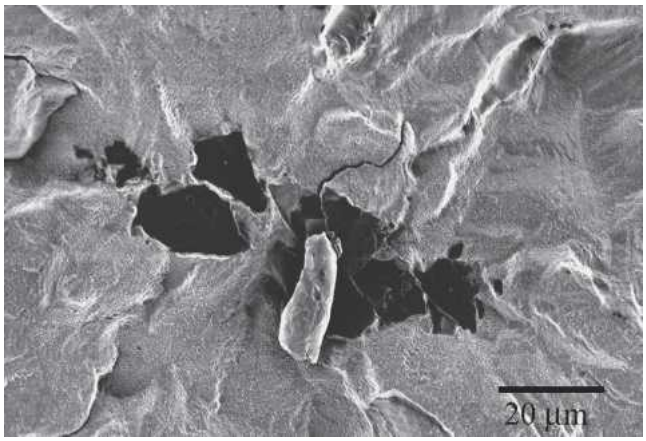

Fig. 7—Higher-magnification image of an inclusion cluster observed in the subsurface of a P condition specimen tested at $\Delta\varepsilon = 0.79$ pct and 650 °C.

factor in determining the crack nucleation mechanism. This is substantiated by the finding that crack nucleation around inclusion clusters was observed only in the small-grain-size P condition specimens and is similar to the conclusions drawn by Alexendre *et al.*,[5] who also found that polycrystalline superalloys become more prone to crack nucleation from inclusions as the material grain size decreases.

In the P condition, at least five of the six specimens tested at $\Delta\varepsilon = 0.66$ pct and $\Delta\varepsilon = 0.79$ pct had dominant cracks that nucleated in the subsurface of the specimen, of which at least four can be directly attributed to inclusions. There were not any obvious inclusions associated with crack nucleation in the fifth specimen exhibiting subsurface crack nucleation. The other specimen exhibited surface slip band crack nucleation. One possible reason for observing subsurface nucleation in the P condition but not the N and O conditions is the difference in volume of material of the LCF specimens between the conditions: the diameter was 10.16 mm for the P condition specimens and 6.35 mm for the N and O condition specimens. The higher volume of material in the P condition specimens means there is a higher probability of the presence of a defect of critical size to nucleate a crack in the specimen. At higher strain ranges ($\Delta\varepsilon = 0.94$ to 1.15 pct), all of the crack nucleation sites could be attributed to slip band damage accumulation. These observations suggest that the crack nucleation mechanism, especially the likelihood of crack nucleation from slip band cracking, is also dependent on the applied strain. This observation will be explored in detail in the next section.

V. MODIFIED FATEMI-SOCIE PARAMETER TO PREDICT CRACK NUCLEATION MECHANISMS

The primary objective of this discussion will be to explain the considerable scatter and disparity observed in LCF properties of nickel-base alloys tested at elevated temperatures based on the possible two crack nucleation mechanisms and, more specifically, using the probability of nucleating a dominant slip band crack. The results indicate how crack nucleation life is greatly affected by microstructural design.

Slip band formation and slip activity become easier as the grain diameter increases, which explains why crack nucleation from slip bands is the only crack nucleation mechanism observed in the N and O conditions compared to the P condition with the much smaller grain size. In addition, cracks that form due to slip band activity within a grain are limited by the grain size until the stress concentration around the crack is sufficient to extend connecting slip bands and cracks into surrounding grains; thus, the largest crack and associated stress intensity within a slip band crack in a grain in the P condition (6-μm grain size) is much smaller than in the N and O conditions (21-μm grain size). Inclusions then become likely candidates for crack nucleation in the P condition specimens, especially at low applied strain ranges and when an inclusion or inclusion cluster is larger than the average grain size. The major dimension of the inclusion clusters observed on P condition fracture surfaces varied between 40 and 120 μm, which is much larger than the average grain size and potential slip band crack. Furthermore, the probability of nucleating a surface slip band crack is very dependent on individual grain size and orientation, which can also produce scatter in the number of cycles required to nucleate a dominant fatigue crack. This physical picture is captured in the model described below, which expands on the work of Fatemi and Socie.[9]

The Fatemi-Socie parameter[9] was developed to predict multiaxial fatigue damage and slip band crack nucleation based on the plastic strain within a slip band and the resolved normal stress to the slip band acting to open a potential crack. The expression for the Fatemi-Socie parameter is

$$\frac{\Delta\gamma^p_{\max}}{2}\left(1 + k * \frac{\sigma_n^{\max}}{\sigma_{ys}^c}\right) \qquad [1]$$

where $\frac{\Delta\gamma^p_{\max}}{2}$ is the maximum plastic shear strain amplitude within the slip band, $\sigma_n^{\max}$ is the peak tensile stress normal to the slip band, σ_{ys}^c is the cyclic yield strength, and $k^* =$ a fitting parameter that has a value of approximately 0.5. The parameter has been equated to a constant, which represents the number of cycles necessary to form a defined crack size, but here it is used as a measure of resistance to crack nucleation, and inferences are made based on these calculations.

Venkataraman *et al.*[10] used strain energy minimization principles to derive the plastic strain within a slip band and the equilibrium slip band spacing for a given strain. They determined that the average plastic shear strain amplitude in a slip band in a single grain γ_p, can be calculated as

$$\gamma_p = 1.39(1 - \upsilon)\left(\frac{\Delta\tau - 2k}{\mu}\right)\frac{d}{w} \qquad [2]$$

where $\nu =$ the Poisson's ratio, $d =$ the effective slip band length or approximately the grain size, $(\Delta\tau - 2k) =$ the shear stress within the slip band minus the frictional resistance, $\mu =$ the shear modulus, and $w =$ the slip band spacing. This expression can be substituted into the Fatemi-Socie

parameter as the maximum plastic shear strain within a slip band.

The resulting model has several appealing features: (1) If grains are considered individually, the model naturally has a dependence on grain orientation; grains oriented favorably for slip have relatively large values of $\Delta\tau$ and thus larger values of the parameter, (2) There is a linear relationship between the Fatemi-Socie parameter and the grain size of the material; the major microstructural difference between conditions N, O, and P is the grain size, and very different crack nucleation mechanisms and fatigue lives have been observed in LCF for the three conditions. The grain size for conditions N and O is more than three times larger than the grain size for condition P, meaning the average Fatemi-Socie parameter will have a larger value for conditions N and O than for condition P and thus predicting that crack nucleation is easier in conditions N and O, and (3) The parameter relies not only on the damage accumulation within the slip band but also the normal stress acting to open a slip band crack, $\sigma_n^{\max}$. This term also allows the parameter to be used for different strain ratios, R, which is essential for comparing the N, O, and P condition data; conditions N and O were fatigue tested with $R = -1$ and condition P was fatigue tested with $R = 0$. Because the P condition specimens were tested with $R = 0$, the mean tensile stress over all the applied strain ranges is higher than the N and O condition specimens tested with $R = -1$. This leads to a larger maximum normal stress applied to a slip band, $\sigma_n^{\max}$, for $R = 0$.

An approximation of slip band spacing was used based on the work of Bailon and Antolovich,[11] who measured slip band spacing in Waspaloy at several applied strain ranges and derived a formula to predict slip band spacing based on applied strain. The grain sizes in conditions N, O, and P are much smaller than the grain sizes studied by Bailon and Antolovich; thus, the slip band spacing should be smaller in the Waspaloy than the Rene 88DT conditions for any applied strain range. However, their results are merely used as an order-of-magnitude approximation for the variation of slip band spacing with applied strain. Since the slip band spacing is inversely proportional to the Fatemi-Socie parameter value, this approximation results in conservative estimates of the Fatemi-Socie parameter. The frictional resistance k was estimated to be one eighth of the shear stress in the slip band, which is a reasonable approximation based on estimates of the internal and frictional components of the shear stress. The resulting expression for the modified Fatemi-Socie parameter incorporating these approximations and Venkataraman's solution for plastic strain within a slip band is:

$$\frac{0.52(1-\nu)}{-3.23\ln\Delta\varepsilon - 11.14}\left(\frac{\Delta\sigma}{M\mu}\right)\left(1+\frac{\sigma_n^{\max}}{2\sigma_{ys}^{c}}\right)d \qquad [3]$$

where $\Delta\sigma$ = the remote applied stress and M = the Taylor factor accounting for grain orientation.

The Fatemi-Socie parameter was used to investigate the probability of slip band cracking in the microstructure conditions N, O, and P on an individual grain-by-grain basis at an intermediate temperature of 650 °C and correlated to experimental results and observations. As a first approximation, a log-normal distribution around the average grain size for each microstructure condition was assumed, with the distribution tails equal to approximately twice the average grain size and half the average grain size, respectively; this is consistent with two-dimensional micrographs of the microstructure. Both γ and γ' are fcc phases, and the dominant slip system in each individual grain at intermediate temperatures was assumed to be in the {111}<110> family. The microstructure conditions have a random texture, so a random distribution of grain orientations was also assumed. Thus, if a force or displacement is applied uniaxially, then the dominant slip system in each grain is also randomly oriented with respect to the loading axis. This scenario was simulated to calculate the distribution of Fatemi-Socie parameter values in individual grains for various applied strain ranges and for the three material conditions. LCF results indicate that the materials have similar stress–strain characteristics, so the only variables that differed in the analysis of the three conditions were the grain size distribution and $\sigma_n^{\max}$ due to the difference in R ratios for each applied strain range.

Figure 8 shows an approximate distribution of the modified Fatemi-Socie parameter for the N and O conditions *vs* the P condition, where the applied strain range is approximately $\Delta\varepsilon = 0.66$ pct. The N and O distribution is larger and there is a higher average value of the Fatemi-Socie parameter than in the P condition. Since the P condition exhibited both nucleation mechanisms and the P condition specimens exhibited relatively long fatigue lives at $\Delta\varepsilon = 0.66$ pct, it can be assumed that a grain must have a comparatively large value of the Fatemi-Socie parameter, which lies toward the tail of the distribution, to nucleate a potentially dominant crack before a dominant crack nucleates from inclusions at this low strain range. If, for example, this is a well-defined value of 0.015, then approximately 7 pct of the grains in the P condition have a Fatemi-Socie parameter value larger than this. Approximately 80 pct of the grains in the N and O conditions have a Fatemi-Socie parameter value that is greater than 0.015. This exercise shows that the number of grains with a critical value of the Fatemi-Socie parameter is far fewer in the P condition than in the N and O conditions. Because of their larger grain sizes, microstructure conditions N and O are much more likely to nucleate slip band cracks. This could account

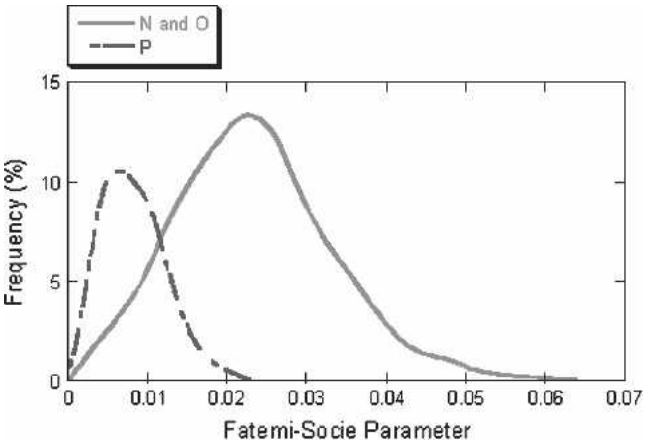

Fig. 8—Approximate distribution of the Fatemi-Socie parameter for the N and O *vs* the P conditions with $\Delta\varepsilon = 0.66$ pct.

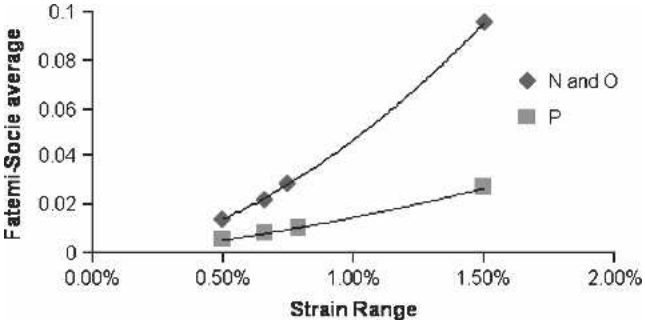

Fig. 9—Average value of the Fatemi-Socie parameter for several strain ranges.

for the considerable differences in fatigue life between conditions N and O *vs* condition P with the much smaller grain size. The exercise also shows that ease of nucleating a dominant slip band fatigue crack is based on the probability of a grain having a critical size and orientation, which can contribute to the scatter in the number of cycles required to nucleate a dominant fatigue crack and in the resulting fatigue lives.

Figure 9 shows a plot of the average Fatemi-Socie parameter for several applied strain ranges for the N, O, and P conditions. Because the tests were strain-controlled, the maximum stress $\sigma_n^{\max}$, in the P condition specimens decreases as the applied strain range increases, and the disparity between the average value of the Fatemi-Socie parameter in the N and O conditions *vs* the P condition increases as the applied strain range increases. The average value of the FS parameter increases approximately as a power law function of strain range, which supports the observation that surface slip band cracking is dominant at larger applied strain ranges. This also complements the notion of the transition strain range defined by Hyzak and Bernstein,[12] who found that surface crack nucleation is more likely to occur above a certain critical strain range and subsurface crack nucleation is more probable below the critical strain range. Slip band crack nucleation always occurs on the specimen surface and is more likely at high strain ranges, whereas crack nucleation from inclusions occurs wherever critically sized inclusions are present, which is more probable in the specimen subsurface. At the largest applied strain ranges ($\Delta\varepsilon = 1.15$ and 1.5 pct), there were multiple surface crack nucleation sites on the fracture surfaces, indicating the ease and higher probability of slip band cracking at higher strain ranges. The Fatemi-Socie calculations complement this observation.

Based on the relationship between the Fatemi-Socie parameter and the likelihood and ease of slip band crack nucleation as verified by experiment, the Fatemi-Socie parameter can be a valuable tool in tailoring microstructures to suppress crack nucleation and increase total fatigue life of structural materials.

VI. CONCLUSIONS

The observations from this study have resulted in the following conclusions:

1. There are two dominant crack nucleation mechanisms prevalent in LCF conditions in Rene 88DT tested at 650 °C. Crack nucleation occurs due to either plastic damage accumulation in persistent slip bands or cracks that originate at inclusion clusters in the subsurface.
2. The average grain size appears to have a major influence on which of the two mechanisms of crack nucleation is present. Subsurface crack nucleation around inclusions is more prevalent for the smaller grain size, whereas the larger grain size favors slip band crack nucleation. The Fatemi-Socie parameter, modified with terms to incorporate grain size and fatigue R-ratio, is a suitable parameter that characterizes the ease of slip band crack nucleation for Rene 88DT material with varying grain sizes.
3. The applied strain range also influences the crack nucleation mechanism, with the higher strain ranges favoring slip band cracking and subsurface crack nucleation occurring more frequently at lower strain ranges, especially in Rene 88DT material with a relatively small average grain size. The Fatemi-Socie parameter complements the notion of a transition strain range above which slip band crack nucleation is favored. This has been borne out by the experimental results of this study as well as by previous researchers Hyzak and Bernstein.[9]
4. The use of the modified Fatemi-Socie parameter can explain the disparity and scatter in fatigue lives observed in the three microstructural conditions tested in this study. It is potentially a valuable tool for tailoring microstructures to suppress crack nucleation and increase overall fatigue life of structural materials.

REFERENCES

1. D.R. Chang, D.D. Krueger, and R.A. Sprague: *Superalloys*, 1984, vol. 1984, pp. 245-73.
2. D.A. Jablonski: *Mater. Sci. Eng. A*, 1981, vol. 48, pp. 189-98.
3. J. Byrne: *Int. J. Fatigue*, 1999, vol. 21, pp. 195-206.
4. M.J. Caton, S.K. Jha, A.H. Rosenberger, and J.M. Larsen: *Superalloys 2004*, 2004, pp. 305-12.
5. F. Alexandre, S. Deyber, and A. Pineau: *Scripta Mater.*, 2004, vol. 50, pp. 25-30.
6. A. Boyd-Lee and J.E. King: *Fatigue and Fracture of Engineering Materials and Structures*, 1994, vol. 17, pp. 1-14.
7. J.C. Healy and L. Grabowski: *Fatigue Fract. Eng. Mater. Struct.*, 1991, vol. 15, pp. 309-21.
8. S. Reichman and D.S. Chang: *Superalloys II*, 1987, pp. 459-93.
9. A. Fatemi and D.F. Socie: *Fatigue Fract. Eng. Mater. Struct.*, 1988, vol. 11, pp. 149-65.
10. G. Venkataraman, Y.W. Chung, and T. Mura: *Acta Metall. Mater.*, 1991, vol. 11, pp. 2621-29.
11. J.P. Bailon and S.D. Antolovich: *Proceedings of the International Conference on Quantitative Measurement of Fatigue Damage*, 1983, pp. 347-49.
12. J.M. Hyzak and I.M. Bernstein: *Metall. Trans. A.*, 1982, vol. 13A., pp. 33-52.